Human-induced oscillations in a network landscape model

Human–induced oscillations in a network landscape model

Rossella Della Marca[1], Maria Groppi[2], Ana Jacinta Soares[3*]

[1]Mathematics Area, SISSA – International School for Advanced Studies,
via Bonomea 265, I-34136 Trieste, Italy
rossella.dellamarca@sissa.it

[2]Department of Mathematical, Physical and Computer Sciences, University of Parma,
Parco Area delle Scienze 53/A, 43124 Parma, Italy
maria.groppi@unipr.it

[3]Centre of Mathematics, University of Minho,
Campus de Gualtar, 4710-057 Braga, Portugal
ajsoares@math.uminho.pt (*corresponding author)

June 9, 2022

Abstract

In this work, we investigate the role of the human factor in the resilience of environmental systems. To this end, a coupled human–landscape model is proposed for a network of Landscape Units (LUs), where each LU is endowed by a system of ODEs for the time evolution of two environmental variables (fraction of green areas and production of bio–energy) and one human variable (fraction of environmentalists in the population). Injunctive social norms that tend to population conformity are taken into account. First the dynamics in each (isolated) LU is analytically investigated, with reference to equilibria and their stability; the possible occurrence of Hopf bifurcations is proved, with consequent periodic oscillations of environmental and human variables, as typical of resilient territories. The numerical investigation shows that such oscillations may disappear by global heteroclinic bifurcations. Then, the connectivity among the LUs is considered, with the aim of pointing out the effects of the single LU dynamics on the network landscape model. Numerical simulations of different scenarios are performed in a sample model of an environmental system in Northern Italy.

Keywords: human–environment system; territorial resilience; Hopf bifurcation; global bifurcation.

1 Introduction

The concept of territorial resilience is closely associated with the ability of a local system to tolerate the impact caused by adverse circumstances and adapt progressively its configuration in order to

support the regional development and the human well–being. See, for instance, [1, 9, 13, 20].

Many factors of different nature, like social instabilities and natural disasters, contribute to weaken the ecological vulnerability of the territories, so that planning activities are needed to provide adequate development policies. The political and societal agenda of the land–use planners can have a crucial impact on the preservation of landscapes and, in particular, of green areas. Both governmental measures and public co–operation are essential in this regard, so that the human behaviour, through environmental policies or opinion movements, plays a significant role in the evolution of landscapes. Additionally, natural reserved areas are rather fragile ecological systems due to the negative impact of climate changes on their natural and ecological value. The threatening implications could compromise these regions and resilient strategies are needed in order to prevent catastrophic effects.

From the mathematical point of view, in dynamical systems ruling the territorial evolution, the convergence of model solutions towards an asymptotically stable stationary state may be considered as a representation of the resilience prompted by a single adverse event (or, at most, a finite number of them). However, very often environmental systems are continuously subject to external disturbances, resulting in the temporal alternation between phases of territorial degradation and phases of reorganization. In such cases, the persistence of the resilience may be more appropriately represented by stable periodic oscillations of the model solutions. Some modelling approaches have been recently proposed in socio and urban planning studies in view of developing management strategies of territorial transformation. See, for example, papers [2, 16] and references cited therein. However, the mathematical models used there are not able to describe resilience by means of oscillating patterns.

In this work, we aim at reproducing the periodic dynamics of the system variables by incorporating the human action in a landscape model. The human behaviour is becoming a key factor in the dynamics of many phenomena in disparate fields. For instance, the spread of infectious diseases is strongly influenced by the voluntary adhesion to vaccination campaigns or to containment measures [6, 7, 21]. Also in the ecological context there are several examples of how humans can change the pathways of an ecosystem. Human activities may lead to a decline in natural ecosystems, the decline in natural ecosystems can in turn stimulate human action to conserve endangered ecosystems or attempt to restore badly damaged ecosystems. Human–environment interactions are a particularly hot topic in the context of forest dynamics, and they have been investigated through various mathematical approaches [3, 10, 11, 18]. A simple differential model for forest dynamics that includes the human factor was presented in [18]; the authors developed a coupled human–environment system where the human population make conservation decisions about a forest ecosystem. In paper [18] two aspects driving human behaviour were examined: conservation priority and injunctive social norms, namely the unwritten but socially acceptable rules and guidelines of a society that tend to support the population conformity.

The complex structure of an environmental system can be modeled by the so–called ecological networks, which are a modern tool to investigate the dynamics of interconnected non–uniform landscape regions (see, for instance, [4, 5]). In this manuscript, we develop a network model by coupling the ecological model proposed in [5] with the human factor. The territory is decomposed in Landscape Units (LUs) and the resulting model is described by a network of dynamical systems, each of them referring to a single node of the network but all sharing the same qualitative structure. Each LU is endowed by a system of ODEs for two variables relevant to the percentage of green areas and to the production of bio–energy, respectively, and by an additional equation for the dynamics of the human action, represented by the fraction of environmentalists in the population, according to [18]. The LUs coupling, namely the connectivity, is realized through the bio–energy exchanges among the LUs.

First, we analytically study the stability properties of the single LU model, determining equilibria and conditions for their existence and stability. In particular, the appearance of limit cycles by Hopf bifurcations is investigated. Moreover, it is numerically shown the possibility of global heteroclinic bifurcations leading to cycles breaking. Then, the effect of the connectivity among the LUs is numerically investigated by simulating the network model, taking as an example an environmental system, already considered in [5], characterized by five LUs where rather compact built–up territorial patches interact with high quality green areas.

The rest of the paper is organized as follows. In Section 2, we present the human–landscape coupled model, with emphasis on the derivation of the equations describing the evolution of the fraction of the environmentalists in the human population, as well as the percentage of green areas and bio–energy production. We present the human–landscape model in each single LU and the relevant network formulation. In Section 3, we perform a qualitative analysis of the single LU model, determining the stationary states and investigating their stability and bifurcations. In Section 4, we perform some numerical simulations in view of investigating the impact of the human behaviour on the stability of the ecological system. We explore different scenarios for both single LU and network models. Finally, in Section 5, we discuss our results and present some concluding remarks.

2 The model

We consider an environmental system consisting of N LUs, that represent different regions separated by natural or anthropic barriers, namely rivers, roads, motorways, railways, buildings, industrial infrastructures, etc.

We are interested in the qualitative evaluation of this environmental system, in terms of three indicators that describe the ecological state of each LU and the impact of the human behaviour in the ecological quality of the environment. These indicators are represented by the normalized state variables $v(t)$, $b(t)$ and $x(t)$ at each time t, where v indicates the green area of the LU with high ecological quality, b measures the biological energy produced by the vegetation inside the LU, and x is the proportion of the environmentalists that work to preserve and protect the green areas.

We derive a human–landscape coupled model describing the time evolution of the state variables v, x, b. For each LU, we establish in Subsection 2.1 the evolution equation for x, by using the theory of evolutionary game dynamics, and we construct in Subsection 2.2 the balance equations for v and b, by incorporating the influence of the environmentalists on the dynamics of the landscape. Then, we propose in Subsection 2.3 the resulting human–landscape model; the network dynamics is also considered, by introducing a connectivity term associated to the interaction among the neighbouring LUs.

2.1 Balance equation for environmentalists

In our model, the human factor can represent opinion movements or political and governmental strategies related to landscape development. In both cases, the human factor influencing the landscape evolution can be modeled by using the evolutionary game dynamics theory (see [21] and references therein). Following [18], we denote by x the proportion of environmentalists in the human population and with $1 - x$ the proportion of non–environmentalists. The imitation dynamics is based on the two strategies (in favor or not in favor of the environment) and individuals may switch between them if the net utility gain for switching is attractive enough. The rate of variation of x is then

proportional to the product $x(1-x)$, related to the contacts between the two population fractions, times the net payoff gain $U_v(v) - U_{av}(v)$ (v being the green area of the LU with high ecological quality), where $U_v(v)$ is the net gain in utility by adopting the environmentalist strategy instead of choosing the anti–environmentalist one, and conversely $U_{av}(v)$ is the net gain in utility by adopting the anti–environmentalist strategy rather than the environmentalist one. Namely, the balance law for the fraction x reads

$$\dot{x} = \kappa' x(1-x)[U_v(v) - U_{av}(v)],$$

where the parameter κ' represents the imitation speed. In addition to the utility gains, individuals in each social group may experience a uniform pressure δ_0 to remain in the same group due to injunctive social norms. Hence, an individual adopting the environmental strategy feels the uniform pressure at the rate $\delta_0 x$ and those adopting the opposite strategy feel the uniform pressure at the rate $\delta_0(1-x)$. By choosing, in addition, $U_{av}(v) = -U_v(v) = q_0 v - r_0(1-v)$ like in [18], we obtain the following equation for x

$$\begin{aligned}\dot{x} &= \kappa' x(1-x)[U_v(v) + \delta_0 x + U_v(v) - \delta_0(1-x)] \\ &= \kappa' x(1-x)[r - mv + \delta_0(2x-1)],\end{aligned}$$

where $r = 2r_0, q = 2q_0$, and $m = r + q$, or equivalently, by factoring out m on the right–hand side,

$$\dot{x} = \kappa x(1-x)[c - v + \delta(2x-1)], \tag{1}$$

with straightforward definition of the parameters κ, c and δ. The parameter c represents the conservation value of green areas, whereas δ represents the pressure due to social norms.

2.2 Balance equations for the environmental variables

The equations describing the evolution of the environmental variables v and b follow the general structure of the ecological models considered in papers [5,14], with the novelty that they incorporate now the influence of the environmentalists in the dynamics. The time evolution of v and b is ruled here by the following equations

$$\begin{aligned}\dot{v} &= dv(1-v) - hUv - s(1-x)v, \\ \dot{b} &= ab(1-b) - l(1-v)b.\end{aligned} \tag{2}$$

Concerning the balance equation for the green areas with high ecological quality inside the LU, v, we assume that the attitude of the non–environmentalists has a direct impact on the degradation of v. Therefore, with respect to the models considered in papers [5,14], the equation for v incorporates a new term represented by $-s(1-x)v$, with s being the human–caused environmental degradation rate, which measures the negative impact of the non–environmentalists towards the green areas [18]. The other loss term, hUv, measures the natural negative impact due to the presence of built–up areas. The coefficient h represents the ratio between the sum of the perimeters of the built–up sectors and the total perimeter of the LU, and $U \in (0,1]$ is the ratio between the sum of the areas of the built–up sectors and the total area of the LU. The coefficient d of the logistic growth depends on solar exposure, relative humidity and ecotonal length (this last quantity is the length of the borders among LUs), and it is an indicator of the ecological quality of the LU. Another minor variation with respect to the models considered in papers [5,14] is that we assume here a pure logistic gain term and neglect its possible dependence on the bio–energy b.

Concerning the balance equation for the biological energy produced by the vegetation inside the LU, b, we assume that the attitude of the environmentalists does not influence directly the evolution of b, but has only an indirect impact on it resulting from the extension of green areas with high quality. Therefore, the evolution equation for b keeps the mathematical structure considered in papers [5, 14]. Such equation describes the balance between the gain term of logistic type with rate a, measuring the solar exposure of the LU, and a typical loss term measuring the negative impact due to the presence of both areas with low ecological quality, represented by $(1 - v)$, and impermeable barriers, represented by the coefficient l, that interfere with the energy flow. In detail, $a \in (0, 1]$ is defined as a weighted average of the areas of the LU exposed to South–East, West and North–East with respect to the total area of the LU, and $l \in (0, 1]$ is the ratio between the surface area of the impermeable barriers included in the LU and the total area of the LU.

2.3 Human–landscape model

In each single LU, the human–landscape model couples equation (1) to (2) and therefore is given by

$$\dot{v} = dv(1 - v) - hUv - s(1 - x)v, \tag{3a}$$
$$\dot{x} = \kappa x(1 - x)[c - v + \delta(2x - 1)], \tag{3b}$$
$$\dot{b} = ab(1 - b) - l(1 - v)b. \tag{3c}$$

Model (3) allows to investigate the impact of the human activities on the dynamics of each LU of the landscape system and their influence on the asymptotic behaviour.

Starting from the single LU model, we construct a network model for the mosaic constituted by $N > 1$ landscape units. Such model is obtained from equations (3), by considering an interaction term in the balance equation for the bio–energy b defining the coupling between each LU of the mosaic and its neighbours. Similarly to what has been done in paper [5], we assume a linear interaction term, which is proportional to the difference between the bio–energies of the LU of interest and all neighbouring LUs. Then, the network model is given by

$$\dot{v}_i = d_i v_i(1 - v_i) - h_i U_i v_i - s_i(1 - x_i)v_i, \tag{4a}$$
$$\dot{x}_i = \kappa_i x_i(1 - x_i)[c_i - v_i + \delta_i(2x_i - 1)], \tag{4b}$$
$$\dot{b}_i = a_i b_i(1 - b_i) - l_i(1 - v_i)b_i + \sum_{j \in \mathcal{I}_i} \gamma_{ji}(b_j - b_i), \tag{4c}$$

where $i \in \mathcal{I}_N$, the set of the indices of all the LUs, and $\mathcal{I}_i$ collects the indices of the LUs neighbouring to the $i-$th one. The connectivity indices γ_{ji} are a measure of the strength of the interconnection between i and j LUs.

The model (4) will be considered in the sequel in view of numerically investigating the effects of the coupling on the evolution of the ecosystem in presence of human actions.

3 Equilibria existence and stability for the single LU model

In this section, we perform a qualitative analysis of system (3). Let us start by noting that the temporal dynamics of the green areas, v, and of the environmentalists, x, is independent from that of

the bio–energies, b. Thus, the investigation of model equilibria can reduce to those of the equations for v and x, namely (3a)–(3b). It is straightforward to check that the region

$$\mathcal{D} = \left\{(v, x) \in [0, 1]^2\right\} \tag{5}$$

is positively invariant for the model system (3a)–(3b), namely each solution with initial conditions in $\mathcal{D}$ remains in $\mathcal{D}$ for all $t > 0$. Hence, it is not restrictive to limit our analyses to this region.

The determination of the equilibria easily follows by setting the right–hand side of system (3a)–(3b) equal to zero and calculating the corresponding solutions. One can verify that the following result holds.

Proposition 1. *System (3a)–(3b) admits five boundary equilibria in the set (5), namely:*

- *an equilibrium of no green areas and no environmentalists*

$$E_0 = (0, 0); \tag{6}$$

- *an equilibrium of green areas and no environmentalists*

$$E_1 = \left(1 - \frac{hU + s}{d}, 0\right), \tag{7}$$

  that exists if $hU + s < d$;

- *an equilibrium of no green areas and full environmentalists*

$$E_2 = (0, 1); \tag{8}$$

- *an equilibrium of green areas and full environmentalists*

$$E_3 = \left(1 - \frac{hU}{d}, 1\right), \tag{9}$$

  that exists if $hU < d$;

- *an equilibrium of no green area and a mix of social ideas*

$$E_4 = \left(0, \frac{\delta - c}{2\delta}\right), \tag{10}$$

  that exists if $\delta > c$.

As far as the equilibria interior to (5) are concerned, system (3a)–(3b) admits a unique interior equilibrium:

$$E_5 = \left(1 + \frac{s(1 - c - \delta) - 2hU\delta}{2d\delta - s}, 1 + \frac{d(1 - c - \delta) - hU}{2d\delta - s}\right), \tag{11}$$

that exists if $-1 < sA + 2\delta B < 0$ and $-1 < dA + B < 0$, with

$$A = \frac{1 - c - \delta}{2d\delta - s} \tag{12}$$

and

$$B = -\frac{hU}{2d\delta - s}. \tag{13}$$

Hence, system (3a)–(3b) admits an equilibrium with green areas and a mix of social ideas (E_5), two equilibria at 'corners' of the set $\mathcal{D}$ (E_0, E_2), and other three equilibria on the boundaries of $\mathcal{D}$ (E_1, E_3, E_4). The equilibrium E_1 exists (namely, it is ecologically meaningful) when the indicator of the ecological quality, d, exceeds the sum of the rate of presence of built–up areas, hU, and the degradation rate, s; this equilibrium represents the possibility that in an LU of 'good' ecological quality the green areas can be present even without environmentalists. The equilibrium E_3 exists when d exceeds only hU, namely, in case of less good ecological quality, the support of the whole population of environmentalists is crucial to support the presence of green areas. The equilibrium E_4 exists when the rate of uniform pressure by injunctive social norms, δ, exceeds the conservation value of green areas, c, and indicates that a suitably high pressure to remain in the same opinion group counteracts the presence of green areas.

Let us denote by

$$E_k = (\bar{v}_k, \bar{x}_k), \ k = 0, \dots, 5,$$

the components of the equilibria. As far as their local stability analysis is concerned, the results are summarized in the following proposition. The acronym LAS stands for 'locally asymptotically stable'.

Proposition 2. *Let us consider the equilibria of system (3a)–(3b), E_k, $k = 0, \dots, 5$, as given in (6)–(11). We assume that they belong to the set $\mathcal{D}$ defined in (5), see Proposition 1. Then,*

- *E_0 is LAS if, and only if, $hU + s > d$ and $c < \delta$;*
- *E_1 is LAS if, and only if, $hU + s < d(1 - c + \delta)$;*
- *E_2 is LAS if, and only if, $hU > d$;*
- *E_3 is LAS if, and only if, $hU > d(1 - c - \delta)$;*
- *E_4 is unstable;*
- *E_5 is LAS if, and only if, $s - 2d\delta > 0$ and $-2\kappa\delta(1 + dA + B)(dA + B) < d(1 + sA + 2\delta B)$, with A and B given in (12)–(13). Furthermore, when $s - 2d\delta > 0$, E_5 undergoes a Hopf bifurcation at $\kappa = \kappa^*$, with κ^* given by*

$$\kappa^* = \frac{d\bar{v}_5}{2\delta\bar{x}_5(1 - \bar{x}_5)}. \tag{14}$$

Proof. By evaluating the Jacobian matrix J of system (3a)–(3b) at each of the equilibrium $E_k = (\bar{v}_k, \bar{x}_k)$, $k = 0, \dots, 5$, one yields:

- $$J(E_0) = \begin{pmatrix} d - hU - s & 0 \\ 0 & \kappa(c - \delta) \end{pmatrix},$$
  implying that E_0 is LAS if, and only if, $hU + s > d$ and $c < \delta$;
- $$J(E_1) = \begin{pmatrix} -d\bar{v}_1 & s\bar{v}_1 \\ 0 & \kappa(c - \delta - \bar{v}_1) \end{pmatrix},$$
  implying that E_1 is LAS if, and only if, $\bar{v}_1 > c - \delta$, namely when $hU + s < d(1 - c + \delta)$;

- $$J(E_2) = \begin{pmatrix} d - hU & 0 \\ 0 & -\kappa(c+\delta) \end{pmatrix},$$

  implying that E_2 is LAS if, and only if, $hU > d$;

- $$J(E_3) = \begin{pmatrix} -d\bar{v}_3 & s\bar{v}_3 \\ 0 & -\kappa(c+\delta-\bar{v}_3) \end{pmatrix},$$

  implying that E_3 is LAS if, and only if, $\bar{v}_3 < c+\delta$, namely when $hU > d(1-c-\delta)$;

- $$J(E_4) = \begin{pmatrix} d - hU - s(1-\bar{x}_4) & 0 \\ -\kappa\bar{x}_4(1-\bar{x}_4) & 2\kappa\delta\bar{x}_4(1-\bar{x}_4) \end{pmatrix},$$

  implying that E_4 is unstable;

- $$J(E_5) = \begin{pmatrix} -d\bar{v}_5 & s\bar{v}_5 \\ -\kappa\bar{x}_5(1-\bar{x}_5) & 2\kappa\delta\bar{x}_5(1-\bar{x}_5) \end{pmatrix},$$

  having $\mathrm{tr}(J(E_5)) = -d\bar{v}_5 + 2\kappa\delta\bar{x}_5(1-\bar{x}_5)$ and $\det(J(E_5)) = \kappa\bar{x}_5(1-\bar{x}_5)\bar{v}_5(s-2d\delta)$. As a consequence, E_5 is LAS if, and only if, $s - 2d\delta > 0$ and $2\kappa\delta\bar{x}_5(1-\bar{x}_5) < d\bar{v}_5$.
  Note that the parameter κ does not affect the existence of E_5, but affects its local stability properties, hence it could be chosen as bifurcation parameter. Let us consider the case that $\det(J(E_5)) > 0$, namely $s - 2d\delta > 0$. Simple algebra yields $\mathrm{tr}^2(J(E_5)) - 4\det(J(E_5)) < 0$ as a 2nd order inequality in κ:

  $$4\delta^2(1-\bar{x}_5)^2\bar{x}_5^2\kappa^2 - \left[4\bar{v}_5(1-\bar{x}_5)\bar{x}_5(s-2d\delta) + 4d\delta\bar{v}_5(1-\bar{x}_5)\bar{x}_5\right]\kappa + d^2\bar{v}_5^2 < 0,$$

  that is satisfied for $\kappa_1 < \kappa < \kappa_2$, with

  $$\kappa_{1,2} = \frac{\bar{v}_5}{2\delta^2\bar{x}_5(1-\bar{x}_5)}\left[s - d\delta \mp \sqrt{s(s-2d\delta)}\right].$$

  Then, Hopf bifurcations occur when $\mathrm{tr}(J(E_5))$ vanishes, namely for $\kappa = \kappa^*$, with κ^* given by (14). It is straightforward to check that $\kappa_1 < \kappa^* < \kappa_2$. Hence, E_5 is an unstable node for $\kappa > \kappa_2$, an unstable focus for $\kappa^* < \kappa < \kappa_2$, a stable focus for $\kappa_1 < \kappa < \kappa^*$, and a stable node for $\kappa < \kappa_1$.

□

In particular, from Proposition 2 it follows that a stationary state of total absence of green areas ($v = 0$) can be LAS in the extreme cases of either full environmentalists (equilibrium E_2) or no environmentalists (equilibrium E_0). In the first case, the stability of this counter–intuitive scenario is justified by the fact that the presence of built–up areas inside the LU, namely the rate hU, is too high in comparison with the solar exposure and relative humidity, represented by d. This does not allow the possibility to improve the ecological quality of the LU if the initial situation is not favorable, even if the whole population is in favor of green areas.

Propositions 1 and 2 do not exclude the possibility that the system (3a)–(3b) admits multiple LAS equilibria at the same time. In particular, bistability can occur between the boundary equilibria

E_0 and E_2 (no green areas with or without environmentalists), E_0 and E_3 (null state and green areas sustained by full environmentalists), E_1 and E_3 (green areas with or without environmentalists), or between E_0 and the interior equilibrium E_5. Specifically, when E_5 is LAS, from $-1 < sA + 2\delta B < 0$ and $-1 < dA + B < 0$, it follows that

$$\frac{hU}{d} < 1 - \frac{s}{2d\delta}(c+\delta) < 1 - c - \delta$$

and

$$\frac{hU+s}{d} > 1 - c + \delta,$$

implying that E_0 can be also LAS, but neither E_1 nor E_2 nor E_3 can.

Also, the local stability analysis predicts the possibility of stationary oscillations arising from a Hopf bifurcation of the interior equilibrium E_5. The presence of oscillations would be significant: oscillating solutions may indicate the territorial resilience to the human action, which results in cycles of degradation/restoration of green areas. We further explore this scenario by numerical simulations in Section 4.

Remark 3. *Once the equilibria E_k, $k = 0, \ldots, 5$, are known, the corresponding stationary values of the production of bio–energy in each LU, b, are obtained by setting the right–hand side of the equation (3c) with $v = \bar{v}_k$ to zero and solving with respect to b. One yields two solutions:*

$$\bar{b}_0 = 0$$

and

$$\bar{b}_{1,k} = 1 - \frac{l}{a}(1 - \bar{v}_k), \tag{15}$$

that exists if $a > l(1 - \bar{v}_k)$. It is straightforward to verify that $\bar{b}_{1,k}$ is an LAS equilibrium for the equation (3c), while $\bar{b}_0$ is LAS if, and only if, $a < l(1-\bar{v}_k)$, namely when $\bar{b}_{1,k}$ does not exist. In other words, when $a-l(1-\bar{v}_k)$ passes from being negative to positive, $\bar{b}_0$ changes its stability character from stable to unstable, and correspondingly the LAS equilibrium $\bar{b}_{1,k}$ emerges. In conclusion, the stability analysis performed for the system (3a)–(3b) is still valid for the full system (3) when considering also the stationary value of b. Accordingly, we maintain the same notation for equilibria also for the full system (3), namely $E_k = (\bar{v}_k, \bar{x}_k, \bar{b}_k)$, with

$$\bar{b}_k = \max\{\bar{b}_0, \bar{b}_{1,k}\}.$$

4 Numerical investigations

In this section, we perform some numerical simulations in view of investigating the impact of the human behaviour on the dynamics of both single LU and network models (3) and (4).

4.1 Parametrization

We refer to landscape data of paper [5]. We select five landscape units like those in [5], with reference to an environmental system located in the northern side of the Turin Province (Italy). Specifically, the choice for these landscape units was motivated by the coexistence and interaction between rather

compact built–up territorial patches and natural reserve areas. The dynamics of v_i, x_i and b_i, $i \in \mathcal{I}_5$, is given at arbitrary time scale [5].

The five LUs are denoted by LU1, LU17, LU18, LU19, LU20, and the set of indices $\mathcal{I}_5 = \{1, 17, 18, 19, 20\}$ is used to label the corresponding parameters and state variables. Table 1 provides

Unit	d_i	h_i	U_i	s_i	κ_i	c_i	δ_i	a_i	l_i	$v_{i,0}$	$x_{i,0}$	$b_{i,0}$
LU1	0.35	1.83	0.09	0.3	1	–	–	0.39	–	0.30	0.5	0.19
LU17	0.26	1.58	0.21	0.3	1	0.01	0.18	0.32	0.11	0.26	0.5	0.13
LU18	0.40	1.97	0.07	0.3	1	–	–	0.44	–	0.31	0.5	0.34
LU19	0.28	1.88	0.61	0.3	1	0.01	0.18	0.31	0.32	0.13	0.5	0.17
LU20	0.26	2.20	0.09	0.3	1	0.10	0.02	0.51	–	0.30	0.5	0.45

Table 1: Baseline values of ecological and human parameters, and initial conditions for numerical simulations of models (3) and (4).

the baseline values of ecological and human parameters, and the initial conditions. Parameter values unspecified in Table 1 are those that vary in the simulation scenarios described below.

The connectivity factors that characterize the interaction among the LUs are grouped in the adjacency matrix $\Gamma = (\gamma_{ij})_{i,j \in \mathcal{I}_5}$, that is given by [5]

$$\Gamma = \begin{pmatrix} 0 & 0.40 & 0.38 & 0 & 0 \\ 0.40 & 0 & 0.63 & 0 & 0 \\ 0.38 & 0.63 & 0 & 0.37 & 0.50 \\ 0 & 0 & 0.37 & 0 & 0.50 \\ 0 & 0 & 0.50 & 0.50 & 0 \end{pmatrix}. \tag{16}$$

The parameter values and the initial conditions that identify the different ecological sectors are taken from [5], where they were obtained from the Geographic Information System measurements [15]. Each LU has some peculiarities. For instance, LU18 and LU20 present initially a good production of bio–energy ($b_{18,0} = 0.34$, $b_{20,0} = 0.45$), together with a rather high value of solar exposure ($a_{18} = 0.44$, $a_{20} = 0.51$). Also, LU20 is characterized by a low presence of built–up areas ($U_{20} = 0.09$), which are strongly dispersed ($h_{20} = 2.20$). Conversely, LU19 has initially a low value of green areas with high ecological quality ($v_{19,0} = 0.13$) and a strong intensity of construction ($U_{19} = 0.61$), which of course implies a high presence of impermeable barriers ($l_{19} = 0.32$). By examining the adjacency matrix Γ it comes out, among others, that the connectivity factor between LU17 and LU19 is equal to zero, indeed these two sectors are completely separated by two contiguous towns. For more details see [5].

For the human parameters and variables, we assume no difference among landscape units in the values of: the degradation rate, that is set to $s_i = 0.3$, $\forall i \in \mathcal{I}_5$; the speed at which opinion change, that is normalized to $\kappa_i = 1$, $\forall i \in \mathcal{I}_5$; and the initial fraction of environmentalists, that is set to half of the total population, $x_{i,0} = 0.5$, $\forall i \in \mathcal{I}_5$. As regards the conservation values of green areas, c_i, $i \in \mathcal{I}_5$, and the rates of uniform pressure to remain in the same group, δ_i, $i \in \mathcal{I}_5$, they are mainly inferred from the bifurcation analyses (see Section 4.2).

Numerical simulations are performed in MATLAB [12]. We use the `ode45` solver for integrating the system of ODEs and the platform–integrated functions for getting the plots.

4.2 Bifurcation diagrams for the single LU model

We start by numerically investigating the asymptotic behaviour of the single LUs, whose analysis has been restricted to the system (3a)–(3b), see Section 3. As anticipated above, we keep all the model parameters fixed except for the human parameters c_i and δ_i, $i \in \mathcal{I}_5$, whose values are inferred from the bifurcation analysis of each LU. Specifically, we are interested in intercepting suitable regions in the parameter space where stationary oscillations are possible for one or more LUs dynamics, with the aim of getting indication on the feasibility of different scenarios of interest for environmental planning. Oscillations are likely to represent the alternation of degradation and restoration of green areas in the environmental system due to both the human action and the territorial resilience.

Note that LU17 and LU19 are characterized by the relation $h_i U_i > d_i$, $i = 17, 19$ (see Table 1, second and fourth lines), indicating that, for such LUs, the benefits of the solar exposure and relative humidity (d) are dominated by the negative impact of the built–up areas (hU). From Propositions 1 and 2, it follows that in this setting the equilibria E_1 (green areas and no environmentalists) and E_3 (green areas and full environmentalists) do not exist, the equilibrium E_2 (no green areas and full environmentalists) is LAS and the interior equilibrium E_5 of coexistence is unstable. Hence, the model solutions can converge either to the equilibrium E_2, or to the equilibrium E_0 (no green areas and no environmentalists) if $c < \delta$, depending on the initial conditions. We consider little significant in our context the scenario in which only the equilibrium E_2 is LAS. Hence, we set c_i, δ_i, $i = 17, 19$, as in Table 1 (second and fourth lines) in order to allow the convergence of LU17 and LU19 dynamics to the equilibrium E_0.

Conversely, LU1, LU18 and LU20 are all characterized by the relation $h_i U_i < d_i$, $i = 1, 18, 20$ (see Table 1, first, third and last lines), indicating that, for such LUs, the benefits of the solar exposure and relative humidity (d) overcomes the negative impact of the built–up areas (hU). From Proposition 2, it follows that in this setting the equilibrium E_2, with no green areas and full environmentalists, is unstable, but a wide variety of asymptotic behaviours is possible. Specifically, for all the three LUs we are considering, with our choice of the degradation rates s_i, it is also $h_i U_i + s_i > d_i$, $i = 1, 18, 20$, which implies that model solutions can converge either to one of the equilibria E_0 (worst scenario of no green areas and no environmentalists), E_3 (green areas in presence of full environmentalists), E_5 (interior), or to a stable limit cycle depending on the relation between c and δ and the initial conditions. But if the direction of the inequality $hU + s > d$ were reversed, namely if the ecological quality of the LU were high enough, one would observe significant variations in the bifurcation diagram of the LU in the plane (c, δ).

For illustrative purposes, a representative bifurcation diagram is given in Fig. 1, left panel [resp. right panel], for the case that $hU + s < d$ [resp. $hU + s > d$]. Unspecified parameter values are those associated to LU18. We observe that when $hU + s < d$, the plane (c, δ) is dominated by the local stability of the equilibria with green areas and no environmentalists (E_1) or with green areas and full environmentalists (E_3), possibly with both simultaneously stable. Specifically, E_1 is LAS for values of (c, δ) above the line $\delta = c - 1 + (hU + s)/d$, E_3 is LAS for values of (c, δ) above the line $\delta = -c + 1 - (hU)/d$. The remaining part of the parameter plane allows for the stability of the interior equilibrium E_5 (Fig. 1, left panel, white region) or predicts the convergence towards stable limit cycles (black region). Indeed, in such black region all equilibria are unstable and the Poincarè–Bendixson theorem [8] allows thus to prove the existence of a stable limit cycle in the invariant squared region $\mathcal{D}$.

When $hU + s > d$ (Fig. 1, right panel), E_1 no longer exists (see Proposition 1) and its position in the bifurcation diagram is covered by the equilibrium of no green areas and no environmentalists

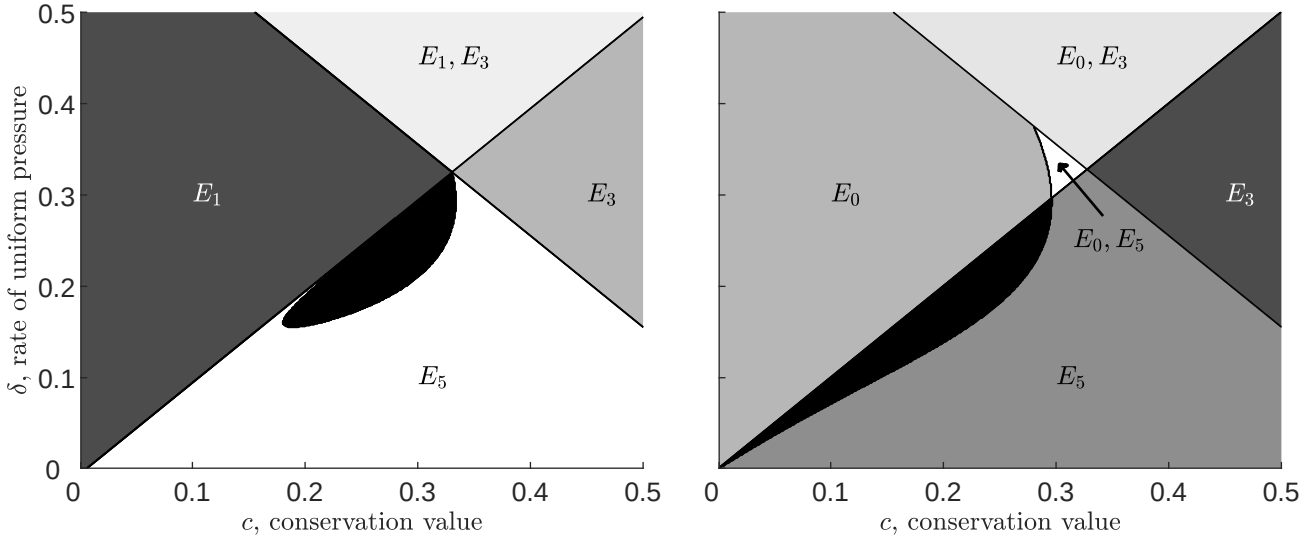

Figure 1: Representative bifurcation diagrams in the plane (c, δ) with reference to LU18. Left panel: case $hU + s < d$ ($s = 0.26$). Right panel: case $hU + s > d$ ($s = 0.30$). The region colour varies according to the type and/or number of equilibria that are locally asymptotically stable. Non–black regions admit one or two locally stable equilibria, as marked in the figure. The black one is the region where all equilibria are unstable and there are stable limit cycles. Unspecified parameter values are those associated to LU18 in Table 1.

(E_0); it means that in LUs where urban settlements and degradation prevail, no green areas can be preserved at the equilibrium in absence of environmentalists. The line $\delta = c$, ruling the stability of E_0, now takes the place of the line $\delta = c - 1 + (hU + s)/d$ ruling the stability of E_1. The region where the interior equilibrium E_5 is LAS expands above the line $\delta = c$, so allowing the bistability between E_0 and E_5 (Fig. 1, right panel, white region). Also, the black region (where all equilibria are unstable and there are stable limit cycles) stretches up to very small values of $c \approx \delta$. This suggests that even for conservation values c near zero, increasing the strength of injunctive social norms, δ, can destabilize the interior equilibrium and generate limit cycles. In general, the amplitude of oscillations increases by increasing δ and the transition between small and large green areas correspondingly becomes more extreme.

Interestingly, from numerical simulations it also turns out that, when $hU + s > d$, in the regions where the equilibrium E_0 is LAS and E_3 is unstable (see Fig. 1, right panel), a *global heteroclinic bifurcation* can occur for a particular set of parameters. Specifically, the limit cycle coalesces with the heteroclinic orbits joining the equilibria E_3 and E_4 (that are saddle points) before disappearing.

We further investigate this phenomenon by setting c and δ in the region where E_0 is LAS and E_3 is unstable and choosing κ as bifurcation parameter (since it may only affect the stability of E_5, but not equilibria existence). More precisely, we set $c = 0.27$, $\delta = 0.30$ and vary κ from 0.6 to 1 (for the case $\kappa = 1$ one can refer to the right panel of Fig. 1). In Fig. 2, we depict the mutual positions of the unstable manifold of the saddle point E_3 (grey lines) and of the stable manifold of the saddle point E_4 (black lines), for $\kappa \in \{0.6, 0.7, 0.75, 0.76, 0.8, 1\}$. In order to approximate such manifolds, we have considered the tangent lines to them obtained from the linearization of the system (3a)–(3b) near the equilibria E_3, E_4. Then we have integrated forward and backward, respectively, taking as initial data small perturbations of the equilibria on those lines. This and other numerical techniques for calculation of heteroclinic cycles are described in [19].

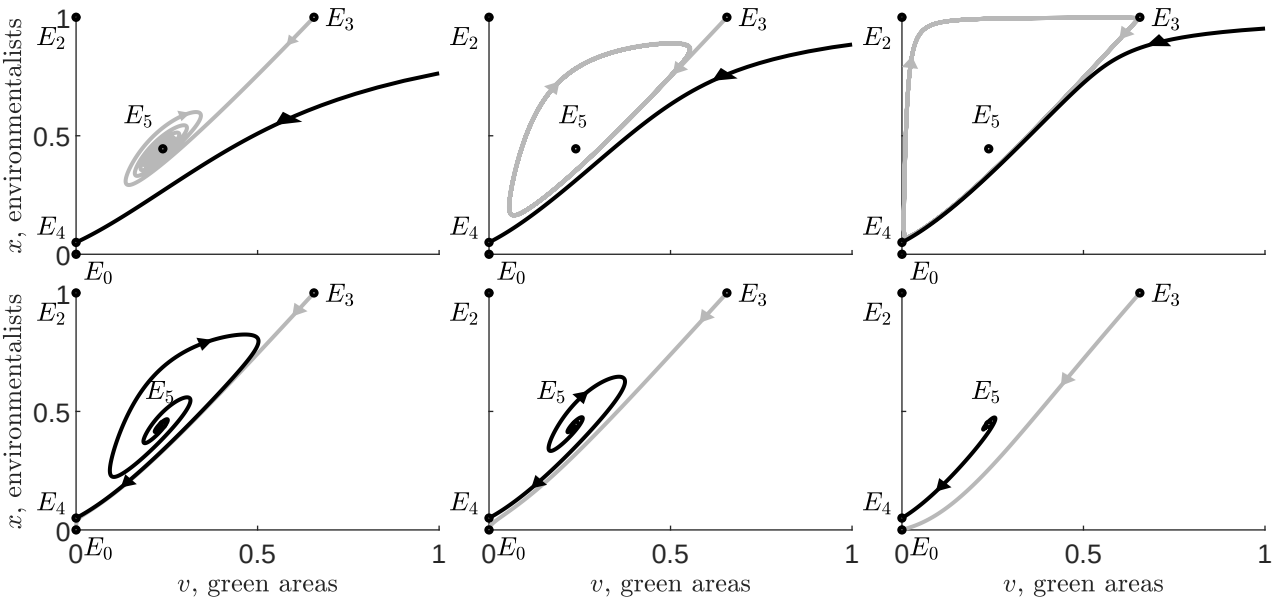

Figure 2: The rise of the global heteroclinic bifurcation. Black [resp. grey] lines denote the stable [resp. unstable] manifold of the equilibrium E_4 [resp. E_3]. Values of the parameter κ from the top left panel to the bottom right panel: 0.6, 0.7, 0.75, 0.76, 0.8, 1. Parameters $c = 0.27$, $\delta = 0.30$. Unspecified parameter values are those associated to LU18 in Table 1.

We can see (Fig. 2) that for $\kappa < 0.75$ (top left and top central panels) the stable manifold of E_4 is below the unstable manifold of E_3. For $\kappa \simeq 0.75$ (top right panel) the two manifolds overlap and a heteroclinic cycle appears (formed by the two heteroclinic orbits joining E_3 and E_4), that coincides also with the limit cycle around E_5, which is present for κ slightly less than 0.75. Then for $\kappa > 0.75$ (bottom panels) the limit cycle disappears, the two manifolds exchange their positions and the unstable manifold of E_3 remains below the stable manifold of E_4. In Fig. 3 the phase portraits before ($\kappa = 0.7$, left panel) and after ($\kappa = 0.8$, right panel) the global bifurcation are shown: in the left panel, trajectories converge either to the equilibrium E_0 or to a limit cycle; in the right panel, the stable limit cycle disappears and all trajectories converge to the null state E_0.

The occurrence of global heteroclinic bifurcations indicates that the stationary oscillations of the model solutions may be not 'structurally stable. Namely, slightly changing the model parameters can lead the limit cycles to break and the oscillations to disappear. In our specific case, this translates into abrupt transitions from a scenario of alternation between relatively small and large areas with high ecological quality inside the LU (due to the alternation between low and high levels of environmentalists in the population) to the total absence of both green areas and environmentalists (equilibrium E_0). This outcome could be interpreted as an effect of the over–exploitation of the natural resources in LUs characterized by $hU + s > d$, namely those where the negative impact of the built–up areas and degradation overcomes the benefits of the solar exposure; this phenomenon is related to the increase of the imitation speed κ. The global bifurcation reveals the existence of a critical value of the parameter κ that can be interpreted as a 'sustainability threshold': when it is overcome, a collapse in the system occurs and high quality green areas degrade rapidly.

4.3 Dynamics of single LU and network models

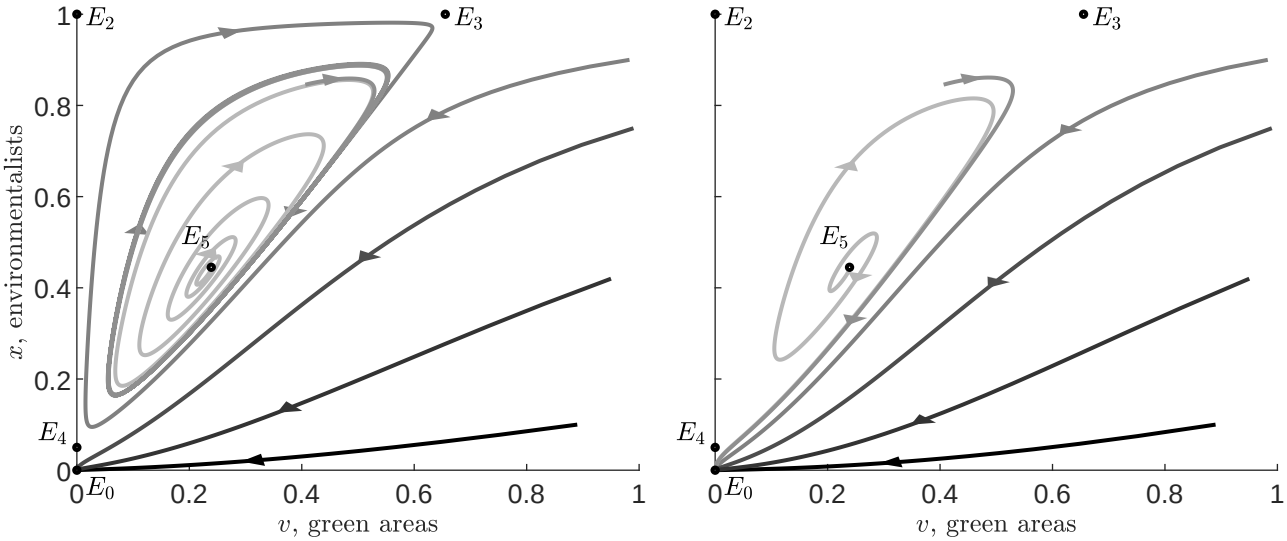

Figure 3: The transition towards the global heteroclinic bifurcation. Phase portraits in the plane (v, x), by assuming a time horizon of [0,3000]. Left panel: $\kappa = 0.7$, trajectories can converge either to the equilibrium E_0 or to a limit cycle. Right panel: $\kappa = 0.8$, the stable limit cycle disappears by collision with the heteroclinic orbit joining equilibria E_3 and E_4 (see also Fig. 2). Parameters $c = 0.27$, $\delta = 0.30$. Unspecified parameter values are those associated to LU18 in Table 1.

The dynamics occurring in the single LUs, discussed in the previous section, are here considered the starting point to plan the simulations of some significant network behaviours. In order to numerically explore different scenarios where stationary oscillations are possible in one or more LUs, we consider the following case studies. Specifically, we set c_i, δ_i, $i = 17, 19$, as in Table 1 (second and fourth lines), in order to ensure the convergence of LU17 and LU19 dynamics to the equilibrium E_0 for the given initial conditions. The parameters c_{20} and δ_{20} are such that the LU20 dynamics converges to the equilibrium E_5 for the given initial conditions (Table 1, last line). Instead, the parameters c_i, δ_i, $i = 1, 18$, vary as follows:

C1 The parameters c_i, δ_i, $i = 1, 18$, are such that the dynamics of the LU1 converges towards a limit cycle and that of LU18 converges to the equilibrium E_5 for the given initial conditions (see Table 2, first line);

C2 The parameters c_i, δ_i, $i = 1, 18$, are such that the dynamics of both LU1 and LU18 converge towards a limit cycle for the given initial conditions (see Table 2, second line).

In both cases, we use the landscape data of paper [5] and the other human parameters as in Table 1. In order to emphasize the role of the impermeable barriers in the dynamics of the landscape model, especially in the oscillating behaviour, we also explore an additional case study, say C2b, that differs from the case study C2 for the values of the parameters related to the presence of impermeable barriers (l) in landscape units LU1, LU18, LU20. Namely, we consider

C2b The parameters c_i, δ_i, $i = 1, 18$, are those in the case study C2, but the parameters l_i, $i = 1, 18, 20$, are greater than those adopted in paper [5] (see Table 2, third line).

Note that in all cases the inequalities $l_i < a_i$, $i = 1, 18, 20$, are satisfied, where a_i are the parameters related to solar exposure.

Case study	c_1	c_{18}	δ_1	δ_{18}	l_1	l_{18}	l_{20}
C1	0.09	0.15	0.08	0.08	0.05	0.04	0.05
C2	0.09	0.17	0.08	0.13	0.05	0.04	0.05
C2b	0.09	0.17	0.08	0.13	0.35	0.34	0.35

Table 2: Landscape units LU1, LU18, LU20. Values assigned to the parameters c_i, δ_i, $i = 1, 18$, and l_i, $i = 1, 18, 20$, in the case study C1 (first line), C2 (second line), C2b (third line).

Dynamics of the isolated LUs. First, we investigate the dynamics of the single human–landscape LU model (3). Temporal dynamics of the solutions to model (3) in the three case studies described above are reported in Figs. 4, 6, 8, respectively (grey lines). The corresponding phase portraits are illustrated in Figs. 5, 7, 9, respectively (grey lines). We notice that, since the bio–energy b_i does not affect the dynamics of v_i and x_i, $i \in \mathcal{I}_5$, the grey lines for these last variables coincide with the black ones relevant to the network dynamics.

In all the case studies, the worst scenarios are those predicted in LU17 and LU19: both the fractions of green areas, v_i, and environmentalists, x_i ($i = 17, 19$), go to the extinction, although at different speeds (the initial percentage of green areas in LU17 is double than that in LU19, see Table 1). The production of bio–energy related to LU19, b_{19}, also approaches the null value, while that related to LU17, b_{17}, settles on the positive stationary value $1 - l_{17}/a_{17} \approx 0.66$, see (15), due to a rate of solar exposure, a_{17}, higher than the presence of impermeable barriers, l_{17}.

As regards the LU20, in all the three case studies, the green areas, v_{20}, and the environmentalists, x_{20}, show damped oscillations towards the respective components of the internal equilibrium E_5, see (11): $\bar{v}_5 \approx 0.12$, $\bar{x}_5 \approx 0.89$. The bio–energy b_{20} also approaches a positive stationary value, namely $\bar{b}_5 = \bar{b}_{1,5}$ (15), but it is much larger in the cases C1 and C2 ($\bar{b}_5 \approx 0.91$) with respect to C2b ($\bar{b}_5 \approx 0.39$) due to the negative impact of the increase of impermeable barriers l_{20} (see Table 2, last column).

Also for the LU1, the dynamics of v_1 and x_1 does not vary in the case studies: it predicts the convergence towards stationary periodic oscillations, representing the alternation of degradation/restoration of green areas due to the corresponding changing in social attitudes. Specifically, the fraction of environmentalists, x_1, oscillates between 0.13 and 0.97 around, and that of green areas, v_1, between 0 and 0.38. In turns, also the bio–energy, b_1, settles on a cyclic regime, but in the cases C1 and C2 it slightly oscillates around a high mean value (≈ 0.88), while in the case C2b, characterized by a higher l_1, the amplitude of oscillations is relatively higher and the mean value is much smaller (≈ 0.18). This behaviour describes a typical pattern of resilient territories, which resist to a human degradation period by regenerating their ecological conditions when the social attitude in favor of the environment increases. The high oscillations observed in the fraction of environmentalists induce moderate oscillations on the percentage of green areas which, in turn, cause very small oscillations on the bio–energy.

Finally, the dynamics of the LU18 is the one that most differs by varying the cases C1, C2 and C2b. In the case C1, v_{18} and x_{18} show an oscillatory behaviour with decreasing amplitude, converging towards the corresponding components of E_5, namely $\bar{v}_5 \approx 0.11$, $\bar{x}_5 \approx 0.28$, and b_{18} converges towards $\bar{b}_5 = \bar{b}_{1,5} \approx 0.92$. The cases C2 and C2b correspond to the scenario of stable stationary oscillations: x_{18} oscillates approximately in the range $(0.07, 0.75)$, v_{18} in the range $(0.03, 0.35)$, while b_{18} slightly oscillates around a high mean value (≈ 0.92) in the case C2, and it oscillates more strongly around a smaller mean value (≈ 0.31) in the case C2b, characterized by a higher l_{18}. Similarly to what happens for the LU1, LU18 shows in the cases C2 and C2b a typical periodic pattern of a resilient territory.

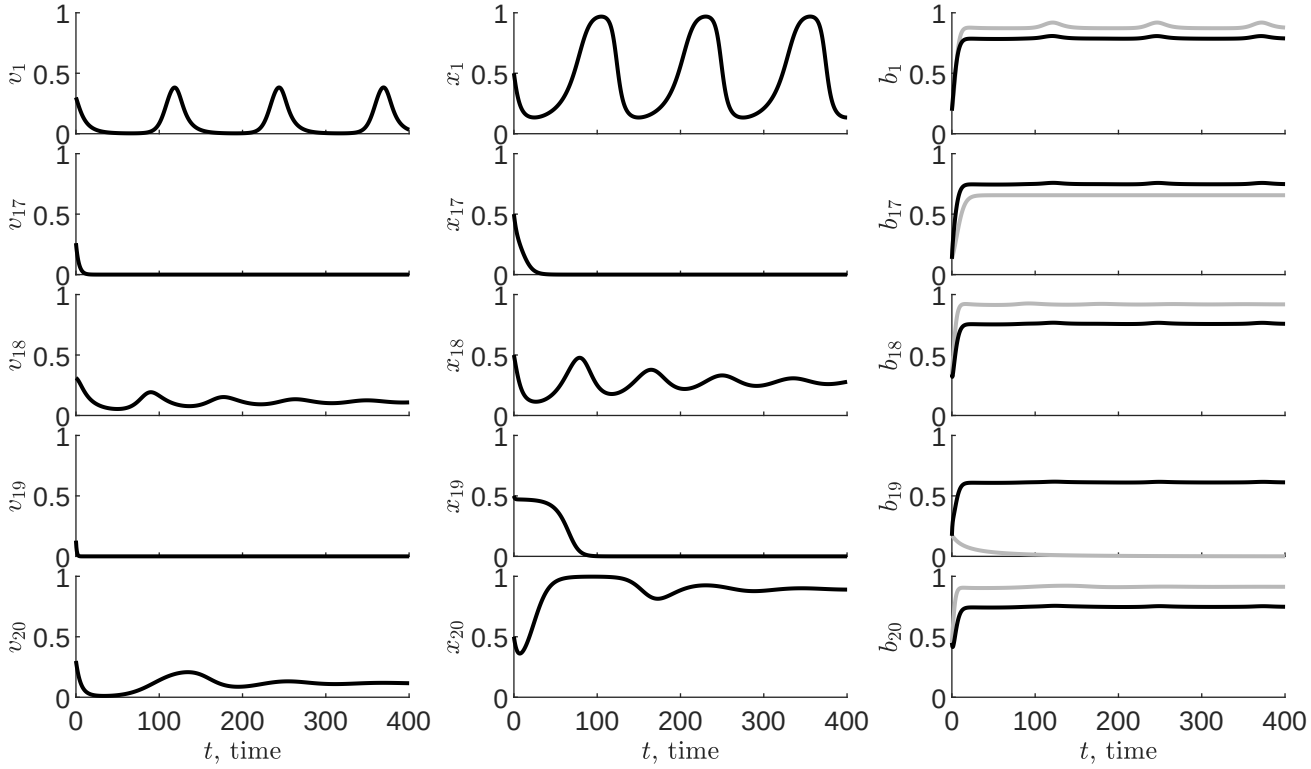

Figure 4: Case study C1. Temporal dynamics of green areas, v_i (left panels), environmentalists, x_i (central panels) and bio–energies, b_i (right panels), for $i \in \mathcal{I}_5$. From the top to the bottom row: LU1, LU17, LU18, LU19, LU20. In right panels, grey [resp. black] lines refer to the dynamics predicted by the single LU model (3) [resp. by the network model (4)]. Parameter values as indicated in Tables 1 and 2.

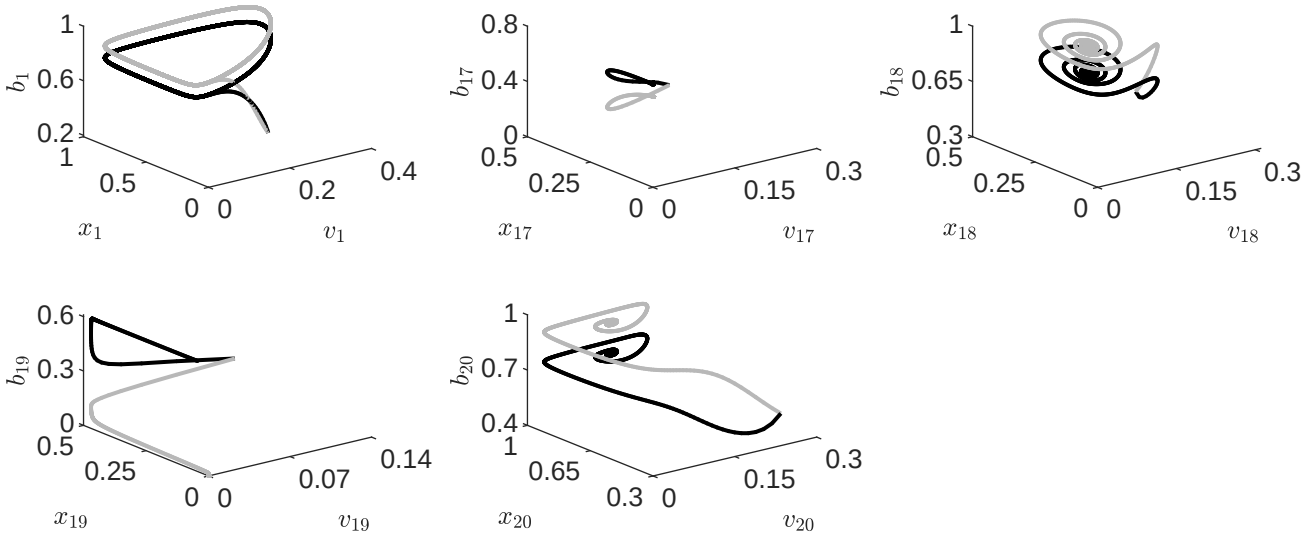

Figure 5: Case study C1. Phase portraits in the space (v_i, x_i, b_i), for $i \in \mathcal{I}_5$, by assuming a time horizon of [0,3000]. From the top left panel to the bottom central panel: LU1, LU17, LU18, LU19, LU20. Grey [resp. black] lines refer to the dynamics predicted by the single LU model (3) [resp. by the network model (4)]. Parameter values as indicated in Tables 1 and 2.

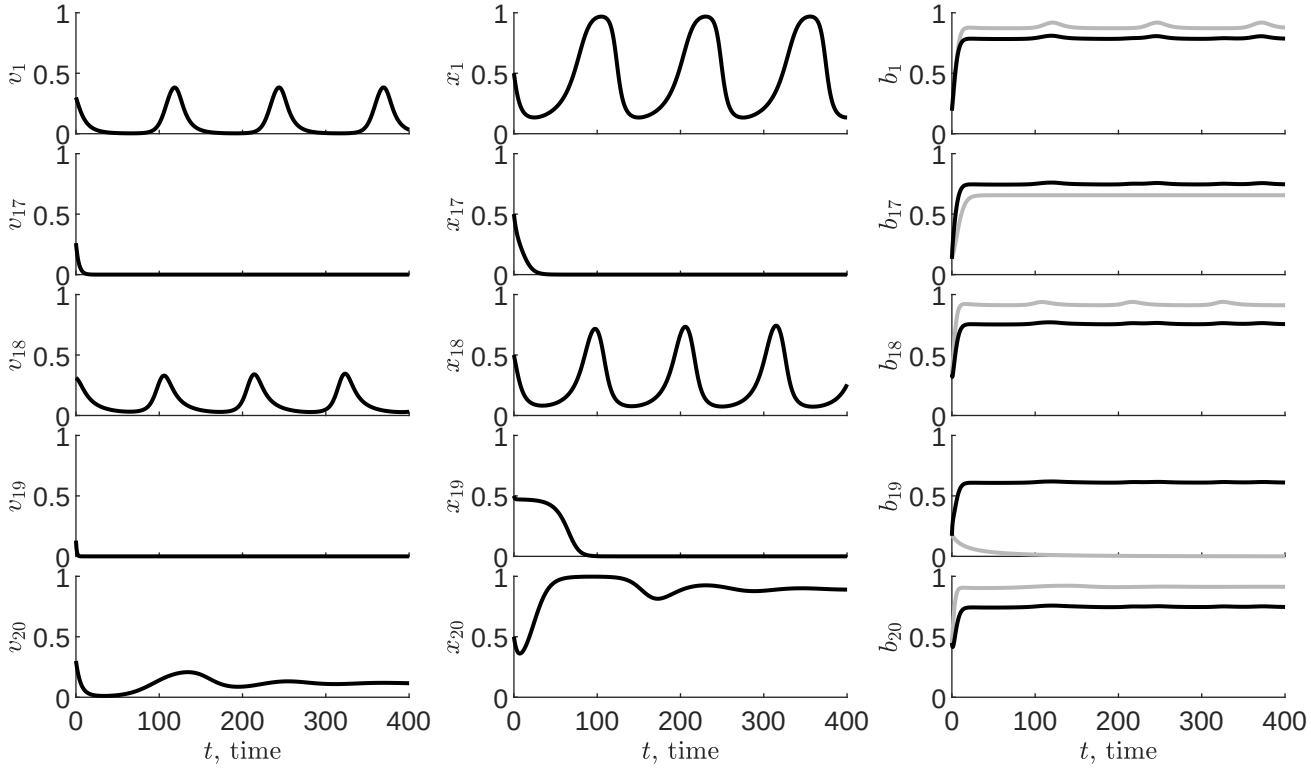

Figure 6: Case study C2. Temporal dynamics of green areas, v_i (left panels), environmentalists, x_i (central panels) and bio–energies, b_i (right panels), for $i \in \mathcal{I}_5$. From the top to the bottom row: LU1, LU17, LU18, LU19, LU20. In right panels, grey [resp. black] lines refer to the dynamics predicted by the single LU model (3) [resp. by the network model (4)]. Parameter values as indicated in Tables 1 and 2.

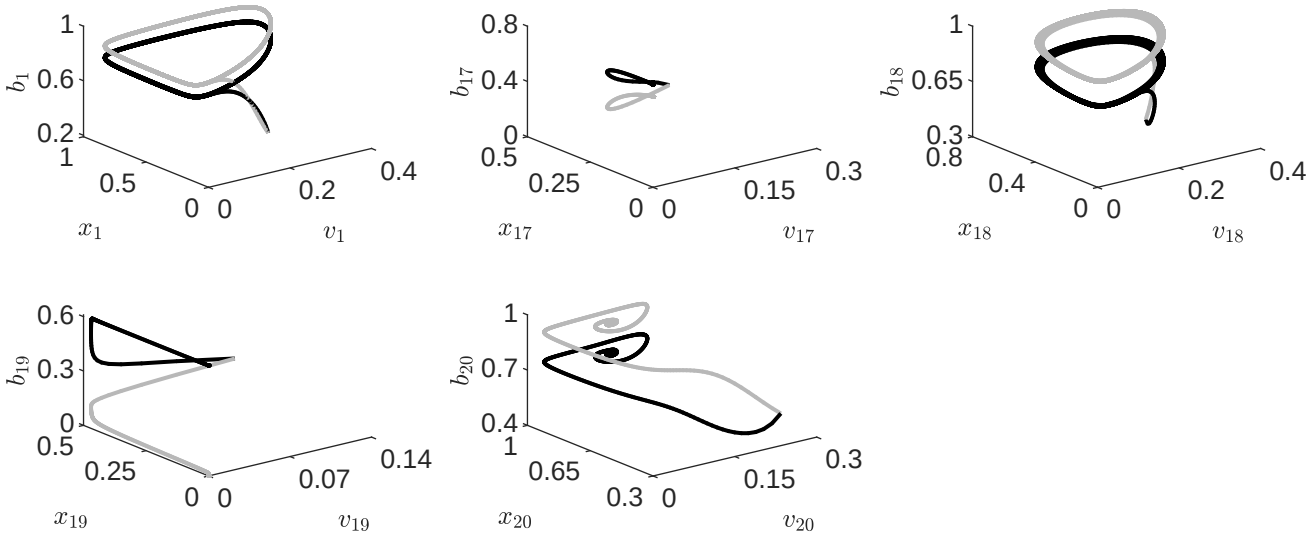

Figure 7: Case study C2. Phase portraits in the space (v_i, x_i, b_i), for $i \in \mathcal{I}_5$, by assuming a time horizon of [0,3000]. From the top left panel to the bottom central panel: LU1, LU17, LU18, LU19, LU20. Grey [resp. black] lines refer to the dynamics predicted by the single LU model (3) [resp. by the network model (4)]. Parameter values as indicated in Tables 1 and 2.

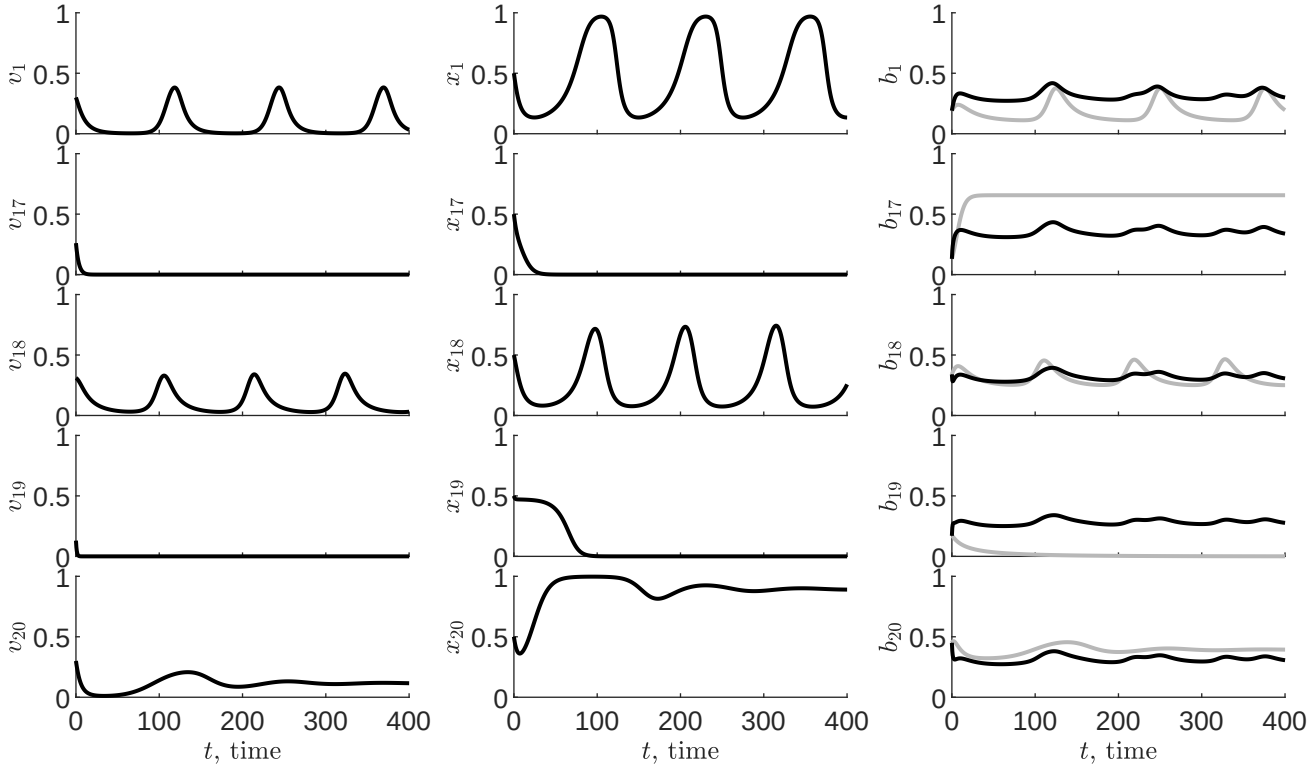

Figure 8: Case study C2b. Temporal dynamics of green areas, v_i (left panels), environmentalists, x_i (central panels) and bio–energies, b_i (right panels), for $i \in \mathcal{I}_5$. From the top to the bottom row: LU1, LU17, LU18, LU19, LU20. In right panels, grey [resp. black] lines refer to the dynamics predicted by the single LU model (3) [resp. by the network model (4)]. Parameter values as indicated in Tables 1 and 2.

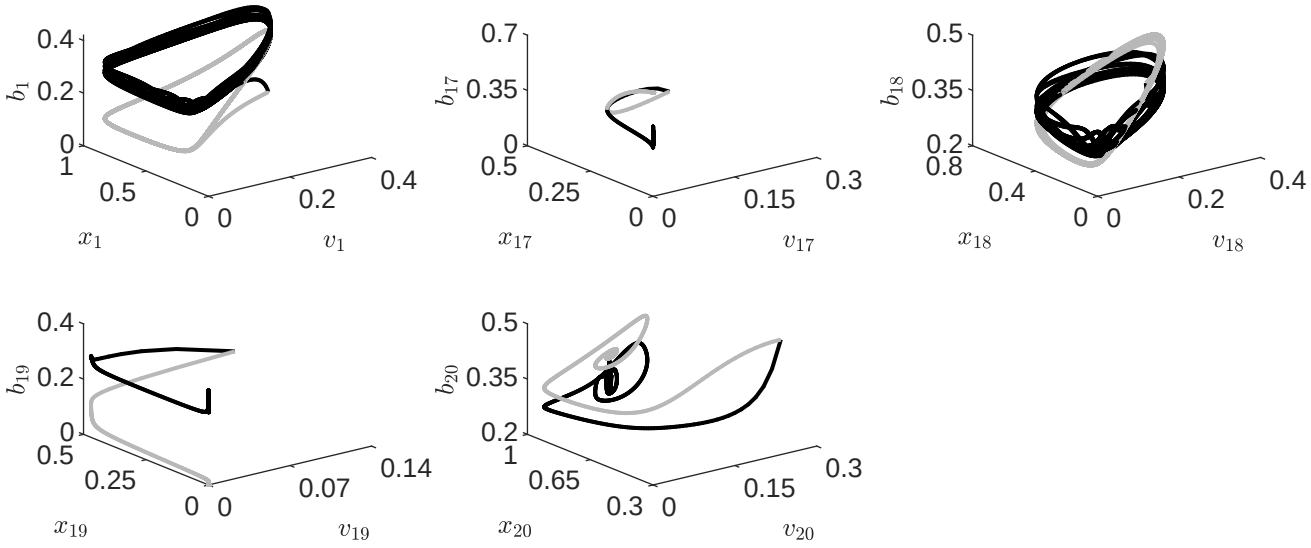

Figure 9: Case study C2b. Phase portraits in the space (v_i, x_i, b_i), for $i \in \mathcal{I}_5$, by assuming a time horizon of [0,3000]. From the top left panel to the bottom central panel: LU1, LU17, LU18, LU19, LU20. Grey [resp. black] lines refer to the dynamics predicted by the single LU model (3) [resp. by the network model (4)]. Parameter values as indicated in Tables 1 and 2.

Network dynamics. Now, we investigate the dynamics of the human–landscape network consisting of the five LUs considered heretofore, but interconnected to each other according to the links ruled by the adjacency matrix (16). Namely, we numerically solve the system (4) by considering the three case studies C1, C2 and C2b, with the aim of analysing the collective dynamics of the network and investigating how the coupling term among the LUs affects the evolution of the system. The corresponding temporal dynamics [resp. phase portraits] are displayed in Figs. 4, 6, 8 [resp. Figs. 5, 7, 9], black lines. We remark that the five LUs interact only through the exchanges of bio–energy b_i, $i \in \mathcal{I}_5$, among them (see equation (4c)).

Generally speaking, we observe that the coupling in the network model modifies in any case the asymptotic production of bio–energy in each LU. In particular, b_i, $i \in \mathcal{I}_5$, assumes an oscillatory trend also in those LUs where oscillations are not predicted by the single LU model. Anyway, the ensuing effect of the network can be either beneficial or deleterious to the LU, in comparison to the isolated case, depending on the ecological conditions of the neighbouring LUs.

Specifically, in the case C1 (Figs. 4 and 5), the network drives the LU17 [resp. LU19] towards a better scenario, characterized by a slightly [resp. widely] higher level of bio–energy. In particular, for LU19, characterized by a high presence of built–up areas (highest value of hU), the network effect allows to pass from null to non–null bio–energy values. On the contrary, the bio–energies of LU1, LU18 and LU20 get worse in the network, settling around a lower level with respect to the isolated case. In all the interconnected LUs, the amplitude of the asymptotic oscillations of b_i, $i \in \mathcal{I}_5$, is minimal (less than 0.02), although little more evident in the LU1 (the only one that exhibits stationary oscillations also when isolated). Similar considerations apply to the case C2 (Figs. 6 and 7), with the only difference of a subtle overall increase in the amplitude of the oscillations of the exchanging b_i's, $i \in \mathcal{I}_5$. Indeed, in such a case, also the dynamics of the single LU18 converges towards a limit cycle.

Radically different is the network dynamics in the case study C2b, characterized by a larger presence of impermeable barriers (Figs. 8 and 9). Here, the coupling in the network model has a beneficial effect on the level of bio–energy in LU1 and LU19, a negative effect on that in LU17 and LU20, but almost no effect on the mean level of b_{18}. In comparison with the cases C1 and C2, the scenario is globally worse: the exchanging b_i's, $i \in \mathcal{I}_5$, exhibit more pronounced and irregular asymptotic oscillations, whose maximum value is in any case even smaller than the minimum value reached in the corresponding cases C1 and C2. This is agreement with the fact that a significant presence of impermeable barriers counteracts the exchange of bio–energy.

5 Discussion and conclusion

In this work, we have developed a new coupled human–landscape model for a mosaic of Landscape Units (LUs). The model consists of a network of interacting dynamical systems, each one describing the behaviour of an LU by means of a system of ODEs for the time evolution of one human variable, the fraction of environmentalists in the LU, and two environmental variables, namely the green areas with high ecological quality and the bio–energy. The interaction among the various dynamical systems is described by a linear term defining the coupling between each LU of the mosaic and its neighbours in terms of the exchanging bio–energy fluxes. The network structure is of paramount importance when investigating, from the ecological point of view, the dynamical properties and asymptotic stability of territories with non–uniform properties. The role of human activities was incorporated into the dynamics as a key factor in view of describing the resilience of environmental

systems in terms of periodic oscillations.

First, we have considered each single LU as an isolated system and studied in detail its own intrinsic dynamics. We have determined the six possible stationary states of the LU, and investigated their stability and bifurcations. In particular, we have observed that stationary periodic oscillations can emerge from a Hopf bifurcation of the internal equilibrium, but the limit cycle can break via a global heteroclinic bifurcation. The wide spectrum of asymptotic configurations indicates that, depending on the initial conditions but also on the magnitude of possible perturbations that affect the territory, the LU can evolve towards very different asymptotic behaviours, also abruptly passing from an oscillatory dynamics to a stationary trend. In particular, a sustainability threshold for the imitation speed κ could exist, at which the over–exploitation of the natural resources causes the sudden degradation of the high quality green areas in LUs with quite poor ecological quality.

We have considered three representative scenarios and implemented some numerical simulations for both the single LU and the network models. Parameter values were chosen so that the dynamics of one or more single LUs converges towards a stable limit cycle, since oscillatory solutions describe the typical pattern of resilient territories that alternate periods of degradation and restoration. The results have shown how the social attitude is crucial to preserve the ecological quality of the environment. In particular, we have observed that, under certain conditions, the fraction of environmentalists exhibits stationary periodic oscillations, which induce periods of degradation of the green areas (when there is a decreasing social attitude towards the protection of the environment) followed by restoration periods in which the territory regenerates its ecological conditions (when there is an increasing social attitude towards the protection of the environment).

Then, we have studied the collective dynamics of the network model by numerically investigating the effects of the LUs coupling on the evolution of the ecosystem. More precisely, we were interested in how the bio–energy of each LU can be affected by that of its neighbouring LUs. Our results show that the network can have either a beneficial or a deleterious impact on the asymptotic bio–energy value of each LU with respect to that predicted by the single LU model. In particular, sectors characterized by a high presence of built–up areas can benefit from the proximity to sectors presenting good levels of green areas and bio–energy. A general outcome is that the coupling term induces an oscillatory trend also in those LUs where oscillations are not predicted when considered isolated.

The results obtained in the present paper corroborate the role played by the connectivity among ecologically different LUs already investigated in [5]. The novelty here is the capability of the new model in reproducing resilience of territories in terms of periodic oscillations and the emphasis on the role of the LUs network in supporting this trend.

The predictions obtained with our model look very reasonable and interesting for what concerns resilience and connectivity, although some simplifications were introduced in order to develop a rather complete mathematical analysis of the model. Therefore, our study presents some limitations, concerning, in particular, the complexity of ecosystems. However, starting from this simple model, some details could be incorporated in order to obtain more accurate predictions. For example, since we are studying a long–term behaviour of the territory, time–dependent model parameters should be more appropriate. Moreover, to take into account possible migrations of people from one region to another in wide areas, a connectivity term depending on the proportion of the environmentalists could be introduced in the balance equation of the green areas. Another interesting problem is the assessment of the impact of invasive plant species on the conservation of natural areas [17]. This could be done by including new terms in the model equations describing the competitive dynamics between the invasive plants and the natural land state. These will be subject of future studies.

Acknowledgements. Fruitful discussions with Professor Roberto Monaco are gratefully acknowledged. Part of this study was carried on during the visiting period of R.D.M. at the Centre of Mathematics of the University of Minho. She wishes to thank the University of Minho for the kind hospitality and the University of Modena and Reggio Emilia for the financial support. The work of A.J.S. is partially supported by the Portuguese FCT Projects UIDB/00013/2020 and UIDP/00013/2020 of CMAT-UM. The work of M.G. is partially supported by the Italian National Research Project *Multiscale phenomena in Continuum Mechanics: singular limits, off–equilibrium and transitions* (PRIN 2017YBKNCE). The present work has been performed under the auspices of the Italian National Group for the Mathematical Physics (GNFM) of National Institute for Advanced Mathematics (INdAM).

References

[1] V. Assumma. *Assessing the Resilience of Socio-Ecological Systems to Shape Scenarios of Territorial Transformation*. PhD thesis, Politecnico di Torino, 2021.

[2] V. Assumma, M. Bottero, E. De Angelis, J. M. Lourenço, R. Monaco, and A. J. Soares. A decision support system for territorial resilience assessment and planning: An application to the Douro Valley (Portugal). *Science of The Total Environment*, 756:143806, 2021.

[3] L.-A. Barlow, J. Cecile, C. T. Bauch, and M. Anand. Modelling interactions between forest pest invasions and human decisions regarding firewood transport restrictions. *PLOS ONE*, 9(4):1–12, 04 2014.

[4] B. K. Bera. Quenching and restoration of oscillations under environmental interactions. *Communications in Nonlinear Science and Numerical Simulation*, 92:105477, 2021.

[5] E. Bonacini, M. Groppi, R. Monaco, A. Soares, and C. Soresina. A network landscape model: stability analysis and numerical tests. *Communications in Nonlinear Science and Numerical Simulation*, 48:569–584, 2017.

[6] B. Buonomo and R. Della Marca. Effects of information–induced behavioural changes during the COVID–19 lockdowns: the case of Italy. *Royal Society Open Science*, 7(10):201635, 2020.

[7] R. Della Marca and A. d'Onofrio. Volatile opinions and optimal control of vaccine awareness campaigns: chaotic behaviour of the forward–backward sweep algorithm vs. heuristic direct optimization. *Communications in Nonlinear Science and Numerical Simulation*, 98:105768, 2021.

[8] M. W. Hirsch, S. Smale, and R. L. Devaney. *Differential Equations, Dynamical Systems, and an Introduction to Chaos*. Academic Press, New York, 2012.

[9] C. S. Holling. Resilience and stability of ecological systems. *Annual Review of Ecology and Systematics*, 4:1–23, 1973.

[10] C. Innes, M. Anand, and C. T. Bauch. The impact of human–environment interactions on the stability of forest–grassland mosaic ecosystems. *Scientific Reports*, 3(1):1–10, 2013.

[11] S. J. Lade, A. Tavoni, S. A. Levin, and M. Schlüter. Regime shifts in a social–ecological system. *Theoretical Ecology*, 6(3):359–372, 2013.

[12] MATLAB. Matlab release 2020a. The MathWorks, Inc., Natick, MA, 2020.

[13] S. Meerow, J. P. Newell, and M. Stults. Defining urban resilience: a review. *Landscape and Urban Planning*, 147:38–49, 2016.

[14] R. Monaco and A. J. Soares. A new mathematical model for environmental monitoring and assessment. In P. Gonçalves and A. J. Soares, editors, *From Particle Systems to Partial Differential Equations*, pages 263–283, Cham, 2017. Springer.

[15] National Geographic. GIS (Geographic Information System). `https://www.nationalgeographic.org/encyclopedia/geographic-information-system-gis/`, 2017. (Accessed on November 2021).

[16] G. Negrini, E. Salizzoni, R. Monaco, A. Soares, and A. Voghera. Inside-outside park planning: a mathematical approach to assess and support the design of ecological connectivity between protected areas and the surrounding landscape. *Ecological Engineering*, 149(105748):1–11, 2020.

[17] T. Ramaj. On the mathematical modelling of competitive invasive weed dynamics. *Bulletin of Mathematical Biology*, 83(13):1–25, 2021.

[18] R. P. Sigdel, M. Anand, and C. T. Bauch. Competition between injunctive social norms and conservation priorities gives rise to complex dynamics in a model of forest growth and opinion dynamics. *Journal of Theoretical Biology*, 432:132–140, 2017.

[19] G. A. van Voorn, L. Hemerik, M. P. Boer, and B. W. Kooi. Heteroclinic orbits indicate overexploitation in predator–prey systems with a strong Allee effect. *Mathematical Biosciences*, 209(2):451–469, 2007.

[20] B. Walker, C. S. Holling, S. R. Carpenter, and A. Kinzig. Resilience, adaptability and transformability in social–ecological systems. *Ecology and Society*, 9:1–9, 2004.

[21] Z. Wang, C. T. Bauch, S. Bhattacharyya, A. d'Onofrio, P. Manfredi, M. Perc, N. Perra, M. Salathé, and D. Zhao. Statistical physics of vaccination. *Physics Reports*, 664:1–113, 2016.